

InGaAs focal plane array with the sub-10 μm pixel pitch and 2.6 μm cut-off wavelength

HE Wei^{1,2,3}, LI Ping^{1,2,3}, SHAO Xiu-Mei^{1,2}, CAO Gao-Qi⁴, YU Yi-Zhen^{1,2}, ZHANG Ya-Guang^{1,2,3},
DENG Shuang-Yan^{1,2}, YANG Bo^{1,2}, LI Xue^{1,2}, LI Tao^{1,2}, GONG Hai-Mei^{1,2*}

(1. State Key Laboratories of Transducer Technology, Shanghai Institute of Technical Physics,
Chinese Academy of Sciences, Shanghai 200083, China;

2. Key Laboratory of Infrared Imaging Materials and Detectors, Shanghai Institute of Technical Physics,
Chinese Academy of Sciences, Shanghai 200083, China;

3. University of Chinese Academy of Sciences, Beijing 100049, China;

4. Fudan University, Shanghai 200433, China)

Abstract: A sub-10 μm InGaAs (IGA) focal plane array (FPA), with cut-off wavelength of 2.6 μm has been developed. The pixel pitch is reduced significantly comparing with that of reported extended wavelength IGA FPAs. To verify the feasibility of technology, the performance of sub-10 μm IGA FPA was tested and compared with 30 μm pixel pitch IGA FPA, which was fabricated from the same epitaxial material. The sub-10 μm IGA FPA exhibits high performances in terms of dark current (0.45 nA @ $V_R = 10$ mV) and R_0A ($14.7 \Omega \cdot \text{cm}^2$) at room temperature. Its quantum efficiency can reach 63%. The comparable performances to 30 μm pixel pitch IGA FPA illustrate that the sub-10 μm IGA FPA fulfils the needs of large formats ($>1 \text{ K} \times 1 \text{ K}$) and high densities in extended wavelength IGA detectors.

Key words: extended wavelength, InGaAs detector, small pixel, dark current density, quantum efficiency

PACS: PACS: 78.30.Fs

中心距 10 μm 截止波长 2.6 μm 的延伸波长 InGaAs 焦平面探测器

何 玮^{1,2,3}, 李 平^{1,2,3}, 邵秀梅^{1,2}, 曹高奇⁴, 于一榛^{1,2}, 张亚光^{1,2,3},
邓双燕^{1,2}, 杨 波^{1,2}, 李 雪^{1,2}, 李 淘^{1,2}, 龚海梅^{1,2*}

(1. 中国科学院上海技术物理研究所 传感技术国家重点实验室, 上海 200083;

2. 中国科学院上海技术物理研究所 红外成像材料与器件重点实验室, 上海 200083;

3. 中国科学院大学, 北京 100049;

4. 复旦大学, 上海 200433)

摘要: 采用 ICP (inductively coupled plasma etching) 刻蚀与湿法腐蚀相结合的方式, 研制了像元中心距为 10 μm 、截止波长 2.6 μm 的 p-i-n 型 10×10 元延伸波长 InGaAs 探测器。不同温度下的电流-电压特性研究和激活能分析, 显示了器件优异的暗电流特性。在室温下, -10 mV 偏压时器件的暗电流和优质因子 R_0A 分别为 0.45 nA 和 $14.7 \Omega \cdot \text{cm}^2$, 量子效率可达到 63%。为了证实像元中心距减小并未影响器件性能, 与同种材料中心距 30 μm 的 InGaAs 焦平面阵列进行了对比分析。相似的实验结果进一步证明了工艺的可行性, 对今后实现高密度、大面阵延伸波长 InGaAs 探测器具有重要的指导意义。

关键词: 延伸波长; InGaAs 探测器; 小像元; 暗电流密度; 量子效率

中图分类号: TN215 文献标识码: A

Received date: 2018-01-31 revised date: 2018-09-28

收稿日期: 2018-01-31, 修回日期: 2018-09-28

Foundation items: Supported by the National Key R&D Program of China (2016YFB0402401), National Natural Science Foundation of China (61376052, 61475179, 61604159)

Biography: HE Wei (1989-), female, Tianshui, China, master. Research area involves semiconductor materials and devices. E-mail: 1684225952@qq.com

* Corresponding author; E-mail: hmgong@mail.sitp.ac.cn

Introduction

Recently, the detector of extended-wavelength InGaAs (IGA) focal plane array (FPA) has attracted great attention, because of its brilliant application prospects in several fields such as defense and security (active imaging), space (earth observation), medicine (disease diagnosis) or industry (non-destructive process control)^[1-2]. Theoretically, the response of lattice-matched $\text{In}_{0.53}\text{Ga}_{0.47}\text{As}$ PIN detectors ranges from 0.9 to 1.7 μm . However, the characteristic absorptions of O-H, C-H, C-O, C=O and N-H mainly range from 1.7 μm to 2.6 μm ^[3], so it is important to develop IGA FPAs with broadband spectrum detection.

High Indium-content $\text{In}_x\text{Ga}_{1-x}\text{As}$ absorbing layers with $\text{InAs}_y\text{P}_{1-y}$, $\text{In}_x\text{Al}_{1-x}\text{As}$, or $\text{In}_x\text{Ga}_{1-x}\text{As}$ linear graded buffers can extend the cut-off wavelength of detectors to 2.6 μm when x reaches 0.8^[4]. But for the reason of difficulty in keeping high performance, caused by lattice-mismatch, the reports on extend wavelength IGA FPA are very limited. The first application of the extended wavelength InGaAs detector was on ESA ENVISAT satellite, its pixel dimension was 25 $\mu\text{m} \times 500 \mu\text{m}$ ^[5]. Later, 320 \times 256 FPA with 30 μm pitches and 2.6 μm cut-off wavelength was fabricated by Judson^[6]. This size of small pixel pitch in extended wavelength IGA detectors had been remained the leading status for a long time. In 2015, an extended wavelength InGaAs detector with 25 μm pixel pitch mesa type had been presented by Y. Arslan *et al.*^[7], with the dark current density of 3.7 $\mu\text{A}/\text{cm}^2$ and R_0A product of $1.96 \times 10^4 \Omega \cdot \text{cm}^2$ ($V_R = 25 \text{ mV}$) at 200 K. Comparing to planar-type IGA FPAs, the progress in mesa-type counterpart for extended wavelength detection is quite slow.

The target for typical planar-type IGA FPAs is about 10 μm pixels size and 2 K \times 2 K format arrays. For example, Teledyne Judson Technologies (TJT) declared in public that they aim to produce < 10 μm pixels and > 2 K \times 2 K format arrays^[8-9]. Therefore, developing small pixel pitches and large formats are also an inevitable trend for extended wavelength IGA detectors.

In this paper, a 10 \times 10 mesa-type extended wavelength IGA FPA is developed with the pixel pitch shortened to 10 μm . The main characteristics including dark current density, responsivity and quantum efficiency are presented and analyzed. To demonstrate the feasibility, the measurement results are also compared with 30 μm pixel pitches extended wavelength IGA FPA's.

1 Experiments

As shown in Fig. 1, the epitaxial structure of the sub-10 μm pixel pitch FPA was consisted of a 0.6 μm $\text{p}^+ \text{In}_{0.83}\text{Al}_{0.17}\text{As}$ top layer, a 1.5 μm $\text{In}_{0.83}\text{Ga}_{0.17}\text{As}$ absorbing layer with unintentional doping level, a 2.0 μm $\text{In}_x\text{Al}_{1-x}\text{As}$ linear graded buffer layer with x changes from 0.53 to 0.8 and a 0.5 μm InP buffer layer. The detector was designed for mesa type and front illumination. The mesas were processed by using inductively coupled plasma (ICP) etching and wet etching. The conductive con-

tacts were obtained through photolithography, etching, evaporation and lift-off. Besides, some tackifier was added into the photoresist, and growth technology of passivation coating was improved during the process of fabrication.

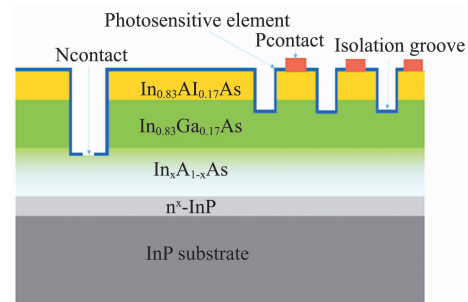


Fig. 1 Schematic illustration of sub-10 μm pixel pitch FPA
图 1 中心矩 10 μm 焦平面阵列器件的结构剖面图

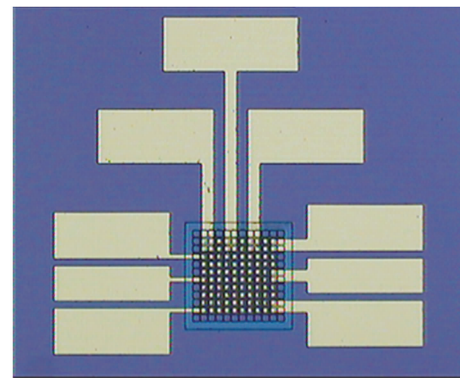


Fig. 2 Optical microscopy image of different pixels chaining by thick electrode pads
图 2 像元电极的引出情况

After fabrication, the wafer was diced into FPAs and connected to circuit for further measurements. To evaluate the performance of a single pixel in details, different number of pixels can be interconnected by Ti/Pt/Au electrodes. The optical microscopy image of the as-fabricated FPA is shown in Fig. 2.

2 Results and discussion

2.1 Morphology of the small pixel device

The micro-morphologies of the sub-10 μm pixel pitch FPA was investigated by using a Supra-55 field emission scanning electron microscopy. In the measurement, the full-chip features and the single pixel morphology were observed. Figure 3 shows the micro-morphologies of the sub-10 μm pixel pitch FPA. The pixel size and pixel pitch are 9 μm and 10 μm respectively. To our best knowledge, this is the smallest size among the reported extended wavelength IGA detectors.

2.2 Dark current mechanism of the device

The temperature dependence of the dark current, which is a key parameter for a detector, has been measured by an Agilent B1500A Semiconductor Device Analyzer. In the measurements, the FPAs were installed into a

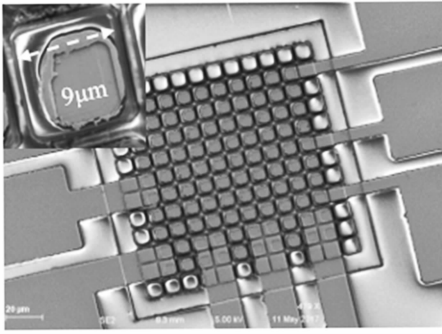


Fig. 3 SEM image of sub-10 μm pixel pitch FPA
图3 中心距 10 μm 焦平面阵列器件形貌的 SEM 表征

dewar assembly and their temperatures were controlled by liquid nitrogen. Figure 4 shows the typical $I - V$ characteristics of a sub-10 μm pixel pitch FPA. The testing voltage was set from -200 mV to 200 mV and the temperature ranges from 220 K to 300 K with an interval of 20 K.

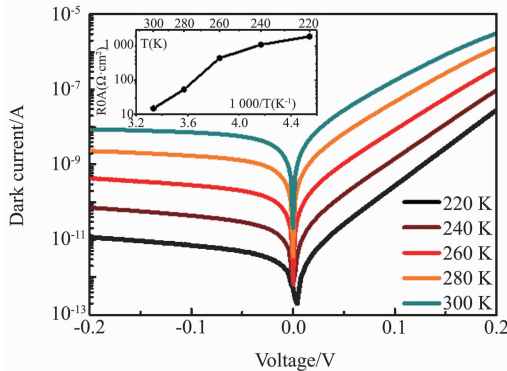


Fig. 4 $I - V$ curves of four $9 \mu\text{m} \times 9 \mu\text{m}$ photodiodes at variable temperatures

图4 4元 $9 \mu\text{m} \times 9 \mu\text{m}$ 光敏元在不同温度的 $I - V$ 特性曲线

It can be seen from Fig. 4 that the dark current of the sub-10 μm pixel pitch FPA is 0.45 nA at 300 K with a reverse bias of $V_R = 10$ mV, and it decreases to 0.5 pA at 220 K. The R_0A is $14.7 \Omega \cdot \text{cm}^2$ (300 K) and $1.96 \times 10^3 \Omega \cdot \text{cm}^2$ (220 K) respectively. These results are superior to many previously reported extended wavelength IGA detectors, such as the $25 \mu\text{m}$ pitch 640×512 format arrays of mesa type IGA FPA^[7]. The lower dark current can be attributed to the improved passivation technique and low lattice defect density of the materials, as our previously reported^[10-11]. The low defect concentration and superior quality of the materials are the one fundamental reason of the favorable dark current. The passivation technique, is a non-negligible factor to suppress the lateral current. In this work, the coating based on SiN_x material is designed to reduce the effects of surface recombination and optimize transmission on spectral band of interest.

Figure 5 gives a comparison between the sub-10 μm pixel pitch FPA and a $30 \mu\text{m}$ pixel pitch FPA,

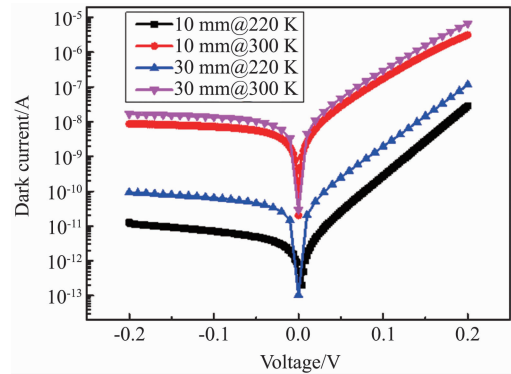


Fig. 5 the contrast of dark current density between sub-10 μm pixel pitch FPA and $30 \mu\text{m}$ pixel pitch FPA

图5 中心距 $10 \mu\text{m}$ 小光敏元器件与中心距 $30 \mu\text{m}$ 器件不同温度下的暗电流密度对比

which was made by the same material. To analyze the relationship between the dark current and temperature, an Arrhenius plot was done at different reverse bias voltages of 10 mV and 100 mV. As shown in Fig. 6, the dark currents, which could be expressed as $I_d \propto \exp(-E_a/KT)$, has two different slopes for the both detectors at the whole range of temperature ($200 \sim 300$ K). In the temperature ranging from 300 K to 250 K, activation energies were deduced at $V_R = 10$ mV for the both sub-10 μm and $30 \mu\text{m}$ pixel pitch FPAs, and they were $E_a = 0.196$ eV and $E_a = 0.177$ eV respectively. It indicates that in this temperature range the internal generation-recombination current and ohmic leakage current is the main source of the dark current. At lower temperature, the dark current drops while the slope becomes lower simultaneously. We also noticed that the surface recombination current of the sub-10 μm pixel pitch FPA is lower than that of the $30 \mu\text{m}$ pixel pitch FPA by comparing their activation energies. The reason is that the depositing condition of the passivation coating is changed to ICPCVD low-rate growth for the sub-10 μm pixel pitch FPA.

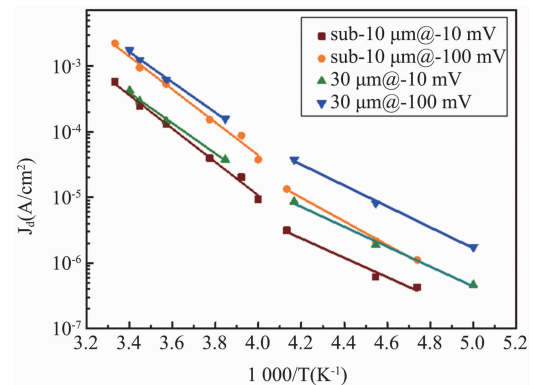


Fig. 6 Arrhenius plot of the dark current versus reciprocal temperature of the detectors at different reverse bias voltage for both sub-10 μm and $30 \mu\text{m}$ pixel pitch FPA

图6 不同反向偏压下中心距 $10 \mu\text{m}$ 小光敏元器件与中心距 $30 \mu\text{m}$ 器件的暗电流机制对比

2.3 Responsivity spectrum and quantum efficiency

The response spectra of both sub-10 μm and 30 μm pixel pitch FPA at room temperature are shown Fig. 7. In the measurement, a Fourier transform infrared (FTIR) spectrometer were used. For both detectors, their illuminate response spectrum and intensity are quite similar except a slight higher response for 30 μm pixel pitch FPA. The main reasons for their difference are two. First, the growth condition and thickness of the passivation film greatly affect the responsivity spectrum^[12]. Second, the increasing area proportion of surface electrodes has affected the absorption of light. The response peak ($\sim 2.30 \mu\text{m}$) and 50% cut-off wavelength ($\sim 2.58 \mu\text{m}$) are essentially the same for both detectors. From the measured results we can also obtain that the responsivity and quantum efficiency of the sub-10 μm pixel pitch FPA are 1.14 A/W and 63% at room temperature respectively. The major performance of the device (sub-10 μm pixel pitch FPA) is summarized in Table 1.

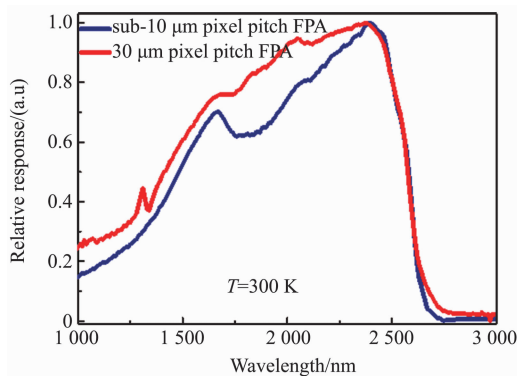


Fig. 7 Relative responsivity spectrum of sub-10 μm and 30 μm pixel pitch FPA at room temperature

图7 中心矩 10 μm 小光敏元器件与中心矩 30 μm 器件室温下的相对响应光谱曲线

Table 1 The major performance of sub-10 μm pixel pitch FPA at room temperature

表1 室温下中心矩 10 μm 小光敏元器件的性能

Pixel area	Dark current density ($V_R = 10 \text{ mV}$)	R_0A	Responsivity	Quantum efficiency
9 $\mu\text{m} \times 9 \mu\text{m}$	$5.72 \times 10^{-4} \text{ A/cm}^2$	14.7 $\Omega \cdot \text{cm}^2$	1.14 A/W	63%

3 Conclusions

The pixel pitch of the FPA presented here is shortened to 10 μm , which reaches the smallest size of InGaAs detector reported in extended wavelength. For the sub-10 μm detector, the typical dark current ($V_R = 10$

mV) and R_0A are 0.45 nA/14.7 $\Omega \cdot \text{cm}^2$ at 300 K, and 0.5 pA/19.6 k $\Omega \cdot \text{cm}^2$ at 220 K respectively. By comparing with 30 μm pixel pitch FPA made of the same material, the desirable dark current and reasonable responsivity verified the feasibility for realizing small pixel pitch FPAs in extend wavelength. Considering the favorable device performance of sub-10 μm with the improved growth technology of passivation coating, this research would provide reference for further study on larger format ($> 1 \text{ K} \times 1 \text{ K}$) InGaAs detectors in extended wavelength area.

Acknowledgement

Authors would like to acknowledge that the material used in this work was supplied by Professor Yong Gang Zhang from Shanghai Institute of Micro-system and Information Technology. And the results of 30 μm pixel pitch FPA was supported by Peng Wei in our group.

References

- [1] Coussement J, Rouvié A, Oubensaid E H, *et al.* New developments on InGaAs focal plane array [J]. *Proc. SPIE*, 2014, **9070** (05): 1–9.
- [2] Rogalski A. Infrared detectors: an overview [J]. *Infrared Physics & Technology*, 2002, **43**:187–210.
- [3] Porod W, Ferry D. Modification of the virtual-crystal approximation for ternary III-V compounds [J]. *Physical Review B*, 1983, **27**: 2587–2589.
- [4] Li X, Gong H M, Fang J X, *et al.* The development of InGaAs short wavelength infrared focal plane arrays with high performance [J]. *Infrared Physics & Technology*, 2017, **80**:112–119.
- [5] Hoogeveen R W, Goede A P. Extended wavelength InGaAs infrared (1.0 ~ 2.4 μm) detector arrays on SCIAMACHY for space-based spectrometry of the Earth atmosphere [J]. *Infrared Physics & Technology*, 2001, **42**:1–16.
- [6] Andresen B F, Yuan H, Fulop G E, *et al.* FPA development: from InGaAs, InSb, to HgCdTe [C]. *Proc. SPIE*, 2008, **6940**: 69403C–1–69403C–10.
- [7] Arslan Y, Oguz F, Besikci C. Extended wavelength SWIR InGaAs focal plane array: Characteristics and limitations [J]. *Infrared Physics & Technology*, 2015, **70**:134–137.
- [8] Rouvié A, Huet O, Hamard S, *et al.* SWIR InGaAs focal plane arrays in France [J]. *Proc. of SPIE*, 2013, **8704**: 870403–1–870403–9.
- [9] Rouvié A, Coussement J, Huet O, *et al.* InGaAs focal plane array developments and perspectives [J]. *Proc. of SPIE*, 2014, **9249**: 92490Z–1–92490Z–8.
- [10] Li P, Li T, Deng S Y, *et al.* Anneal treatment to improve the performance of extended wavelength In_{0.83}Ga_{0.17}As photodetectors [J], *Infrared Physics & Technology*, 2015, **71**: 140–143.
- [11] Zhang Y G, Gu Y, Zhu C, *et al.* Gas source MBE grown wavelength extended 2.2 and 2.5 μm InGaAs PIN photodetectors [J]. *Infrared Physics & Technology*, 2006, **47**: 257–262.
- [12] Dhar N K, Dutta A K, Tao L, *et al.* Responsivity performance of extended wavelength InGaAs shortwave infrared detector arrays [J]. *Proc. SPIE*, 2014, **9100**: 9100U–1–9100U–7.